An obese brain and an inflamed body: Central and peripheral consequences of obesity

de Weijer, B.A.M.

Publication date
2016

Document Version
Final published version

8

Morbid obesity is associated with hepatic inflammation independent of liver fat content and insulin sensitivity

Barbara A. de Weijer, Marco van Eijk, Mariëtte T. Ackermans, Joanna Verheij, Ignace Janssen, Frits Berends, Arnold van de Laar, Lex P. J. Houdijk, E. Fliers, Aart J Nederveen and Mireille J. Serlie

Submitted

Abstract

Background: Obesity is associated with hepatic steatosis, hepatic insulin resistance and low-grade inflammation. Liver inflammatory markers, insulin resistance and liver fat were shown to be associated in obese animal models of NAFLD. Whether inflammation and liver fat contribute to hepatic insulin resistance in obese humans is controversial.

Methods: We studied insulin sensitivity during a two-step hyperinsulinemic euglycemic clamp with a stable glucose isotope tracer in 20 obese women (41 [26-58] yrs.; body mass index (BMI) 45.3 [39-61] kg/m2) undergoing bariatric surgery. Gene expression of inflammatory markers in liver biopsies were compared to expression levels in liver biopsies from 6 lean glucose tolerant matched controls (36 [26-45] yrs.; BMI 22 [20-24] kg/m2) scheduled for elective cholecystectomy. Intrahepatic triglycerides (IHTG) were assessed in the obese women using ^{1}H-MR Spectroscopy (^{1}H-MRS) and liver biopsies were scored for steatosis and non-alcoholic fatty liver disease (NAFLD) activity.

Results: Mean IHTG was 7.7 ± 9.0% [range 0-28.8%] and one of the subjects showed histological signs of non-alcoholic steatohepatitis (NASH). Liver expression levels of pro- and anti-inflammatory markers along with CD68 were markedly increased in the obese patients compared to the controls. Within the obese group with liver steatosis, IL10 inversely correlated with liver fat content. None of the other inflammatory markers predicted liver fat content, basal endogenous glucose production (EGP) or hepatic and peripheral insulin sensitivity. IHTG did not correlate with hepatic or peripheral insulin resistance.

Conclusions: In conclusion, in morbidly obese women, the liver is inflamed independent of intrahepatic triglycerides and hepatic insulin sensitivity. This suggests that stored triglycerides do not promote inflammation or insulin resistance per se and that liver inflammatory changes in the absence of NASH do not contribute to insulin resistance.

Introduction

Obesity is associated with hepatic steatosis, hepatic insulin resistance and low-grade inflammation (1, 2). Growing evidence shows that these metabolic conditions are intertwined and contribute to the development of type 2 diabetes mellitus (DM2) and non-alcoholic fatty liver disease (NAFLD) (3). NAFLD represents a state of excessive triglyceride accumulation in the liver, which may progress to non-alcoholic steatohepatitis (NASH) and finally hepatic cirrhosis and end stage liver disease (4). The etiology of hepatic steatosis in obesity includes increased portal delivery of free fatty acids (FFA), reduced beta-oxidation and increased de novo lipogenesis (5, 6). In obese patients with DM2 liver fat content is increased and is accompanied by impaired insulin clearance and hepatic insulin resistance (7). Although the relation between liver fat and insulin resistance has been demonstrated in rodents and humans, the pathophysiological mechanism is only partly elucidated. We previously showed that insulin sensitivity in subjects with familial hypobetalipoproteinaemia and severe liver steatosis was comparable to matched controls without hepatic steatosis (8) suggesting that intrahepatic triglycerides per se do not cause hepatic insulin resistance. Instead, a major role for diacylglycerol with subsequent activation of protein kinase C (PKC) has been described (9, 10).

Another characteristic of obesity-associated insulin resistance is inflammation. Whether liver inflammation in the setting of obesity contributes to hepatic steatosis or hepatic insulin resistance is currently unknown. Inflammatory changes in NAFLD have been attributed to a reduction in peroxisome proliferator-activated receptor ɣ (PPARɣ) expression, lower circulating adiponectin, exposure to cytokines derived from adipose tissue as well as lipotoxicity induced by fatty acid overload (11, 12). Moreover lipid-induced endoplasmic reticulum (ER) stress has been associated with insulin resistance in mice (13) and recently heme oxygenase-1 has been proposed as a pro-inflammatory signal linking inflammation to insulin resistance in mice on a high fat diet (14). Finally, Kupffer cells (the resident macrophages of the liver) decrease in rodents on a high fat diet while recruited myeloid cells invade the liver through a mechanism involving the C-C chemokine receptor type 2 (CCR2). Subsequently the invaded immune cells trigger hepatic fat accumulation which is dependent on chemokine (C-C motif) ligand 2 (CCL2)/CCR2 (15). In support, short term infusion of oleate increases hepatic recruitment of myeloid cells, suggesting that increased portal delivery of FFA both induces inflammation and triglyceride (TG) accumulation through induction of chemotaxis (15). These findings in animals suggest a complex interplay between diet and obesity- associated inflammation, hepatic fat accumulation and insulin resistance. To study the relation between liver inflammation, hepatic fat content and hepatic insulin sensitivity in humans, we studied morbidly obese women with a wide range in hepatic fat content and assessed glucose metabolism, intrahepatic triglycerides (IHTG) and expression profiles of inflammatory markers in liver biopsies. The expression profiles were compared to matched lean and glucose tolerant controls.

Subjects and methods

Subjects

Twenty morbidly obese women scheduled for Roux-en-Y gastric bypass surgery (RYGB) and six healthy lean women scheduled for elective cholecystectomy for benign gallbladder disease were included. Subjects were recruited from the outpatient clinics of the Rijnstate Hospital in Arnhem, the Slotervaart Hospital in Amsterdam and the Medical Center Alkmaar in Alkmaar.

The obese patients were eligible to participate if they were scheduled to undergo RYGB surgery, were older than 18 years, understood the objective of the study, and were competent to give informed consent. Exclusion criteria were: childhood onset obesity, insulin dependent DM2, coagulation disorders, a recent history (6 months or less) of alcohol or drug abuse; the use of antipsychotic medication or antidepressant medication; any somatic illness except for obesity-related conditions (hypertension, dyslipidemia and DM2 treated with oral anti-diabetics); Inclusion criteria for the lean controls were: body mass index (BMI) < 25 kg/m2, scheduled for elective cholecystectomy for benign gallbladder disease. Exclusion criteria were any other medical condition, coagulation disorders, glucose intolerance and use of any medication. Glucose tolerance was assessed during a 75 g oral glucose tolerance test in the lean controls.

The study was approved by the Medical Ethical Committee of the Academic Medical Center (AMC) of the University of Amsterdam. After a complete description of the study had been given, written informed consent was obtained.

Hyperinsulinemic euglycemic clamp

The obese women participated in a study on the short-term metabolic effects of bariatric surgery (16). Two weeks before surgery, they were admitted to the Metabolic Clinical Research Unit of the AMC after an overnight fast and were studied in the supine position. A catheter was inserted into the dorsal vein of the hand or distal vein of each arm. One catheter was used for sampling of arterialized blood using a heated hand box (60°C). The other catheter was used for infusion of [6,6-$^2H_2$]glucose, glucose 20%, and insulin. At T=09:00 h (T= -2h), after drawing a blood sample for background enrichment of plasma glucose, a continuous infusion of [6,6-$^2H_2$]glucose (99% enrichment; Cambridge Isotopes, Andover, MA) was started at a rate of 0.11 µmol/kg*min after a priming dose equivalent to 120 minutes infusion. After 110, 115 and 120 min, blood samples were drawn for determination of glucose enrichments, glucoregulatory hormones and FFA. Subsequently, at T=11:05 h (T=0:05), a continuous infusion of insulin (Actrapid 100U/ml; Novo Nordisk Farma, Alphen a/d Rijn, the Netherlands) was started for 2h at a rate of 20 mU/m^2 body surface area min^{-1}. At T=2h, the infusion rate of insulin was increased to 60mU/m^2 body surface area min^{-1}. Plasma glucose was measured every 10 min and glucose 20% was infused at a variable rate to maintain plasma glucose at 5.0 mmol/L. [6,6-$^2H_2$]glucose was added to the 20% glucose solution to achieve glucose enrichments

of 1% to minimize changes in isotopic enrichment due to changes in the infusion rate of exogenous glucose. At T=2h and T=4h, 5 blood samples with a 5 minutes interval were drawn to measure glucose enrichments and 2 samples were drawn to measure glucoregulatory hormones and FFA. During the study the participants were allowed to drink water only.

Analytical procedures

Plasma glucose concentrations were measured with the glucose oxidase method using a Biosen C-line plus glucose analyzer (EKF Diagnostics, Barbleben/Magdeburg, Germany). Plasma FFA concentrations were determined with an enzymatic colorimetric method (NEFA-C test kit; Wako Chemicals, Neuss, Germany) with an intra-assay variation of 1%, inter-assay variation of 4-15% and a detection limit of 0.02 mmol/L. [6,6-$^{2}H_{2}$]glucose enrichment (tracer-to-tracee ratio) was measured as described earlier (17). Insulin and cortisol were determined on an Immulite 2000 system (Diagnostic Products, Los Angeles, CA, USA). Insulin was measured with a chemiluminescent immunometric assay with intra-assay variation of 4–5%, inter-assay variation of 5% and detection limit of 15 pmol/l. Cortisol was measured with a chemiluminescent immunoassay with an intra-assay variation of 3-6%, inter-assay variation of 5-7% and a detection limit of 50 nmol/l. Glucagon was determined with the Linco 125I RIA (Linco Research, St Charles, MO, USA) with an intra-assay variation of 4-8%, inter-assay variation of 6-11% and detection limit of 15 ng/l.
C-reactive protein (CRP) was determined using ELISA (R&D systems Europe, Ltd. Abingdon, UK), according to the manufacturer's instructions.

Intrahepatic triglycerides (^{1}H– Magnetic Resonance Spectroscopy (^{1}H–MRS))

In the obese subjects, ^{1}H-MRS measurements were performed two weeks before surgery on an open 1.0 Tesla Magnetic Resonance (MR) scanner with a 160 cm-wide patient aperture and a height of 45 cm (Panorama HFO, Philips Healthcare, Best, The Netherlands) using the body coil in supine position (total scan time including localizers 30 minutes). A 20 x 20 x 20 mm voxel was positioned in the right liver lobe and a voxel was positioned left, avoiding overlap with extrahepatic structures and intrahepatic vascular and biliary structures. IHTG was determined from the mean of these two voxels.
Spectra were acquired using first order iterative shimming, a point resolved spectroscopic sequence (PRESS) with TE/TR=35/2000 ms and 64 signal acquisitions. Data was processed using jMRUI software (18). Signal resonances from water and fat located at 4.65 and 1.3 ppm respectively were analyzed. Prior knowledge was used for peak localization by using soft constraints. Signal resonances were fitted using Lorentzian line shapes. Phase variation was allowed (40 degrees) around a manually selected optimum. Relative fat content was expressed as a ratio of the fat peak area over the cumulative water and fat peak areas (1.3 ppm / (1.3 ppm + 4.65 ppm). No correction for T1 relaxation was performed, as T1-weighting is negligible at 1.0 Tesla using a TR of 2000 ms. Calculated peak areas of water and fat were corrected for T2 relaxation. T2 measurements were performed in all patients by using a

multi echo PRESS (TE= 40, 70, 100, 130 and 160 ms). The T2 measurements were used for calculating the weight percentage IHTG according to Szczepaniak et al (19).

Body composition

Body composition was measured using bioelectrical impedance analysis (Maltron BF-906, Rayleigh, UK).

Surgical procedure and tissue biopsies.

The surgical procedures were carried out in three medical centers (Rijnstate Hospital, Arnhem, Slotervaart Hospital, Amsterdam and the Medical Center Alkmaar, Alkmaar) and performed by experienced surgeons. During surgery, liver biopsies were taken at the beginning of the surgical procedure. Hemostasis was checked directly after the biopsies and at the end of the surgical procedure. Samples were taken from similar locations in all patients of segment 3 of the liver, and at the same time point during surgery. Part of the tissue was snapfrozen in liquid nitrogen, and thereafter stored in -80ºC for subsequent analysis. Another part of the tissue was fixed in buffered formalin and subsequently paraffin embedded.
Total RNA was extracted from the frozen biopsies using TRIzol reagent (Invitrogen), followed by further extraction using the NucleoSpin RNA II kit according to the manufacturer's recommendations (Macherey-Nagel GmbH, Duren, Germany). This protocol included a RNase-free DNase step. RNA concentrations were determined using a Nanodrop Spectrophotometer (Nanodrop Technologies, Wilmington, DE, USA). RNA integrity was investigated by assessing the RNA integrity number (RIN), using an Agilent 2100 Bioanalyzer (Agilent Technologies, Waldbronn, Germany); mean RIN numbers were 7.
Equal amounts of RNA were used to synthesize cDNA, using oligo-$(dT)_{12-18}$ and random hexamers as primers, and Superscript II reverse transcriptase, according to the manufacturer's method (Invitrogen). Gene-specific analysis was performed on an iCycler MyiQ single-color real-time PCR detection system using iQ SYBR Green Supermix (Bio-Rad Laboratories). Gene expression levels were normalized to the acidic ribosomal protein *36B4, also referred to as P0.* The following primers were used: CD68, CD163, Mannose receptor (MR) , CCL2 (the primary ligand of CCR2), Tumor necrosis factor alpha (TNFα) , macrophage inflammatory protein (MIP1β) and interleukin 10 (IL10). The primer sequences are shown in a supplemental table. Specificity of the primers was verified by evaluation of the amplifications with the use of gel electrophoresis and melting curve analysis.

Histopathology liver

Liver specimens were routinely formalin-fixed and paraffin-embedded. For scoring, a hematoxylin and eosin and a Sirius Red stain were available. Sections were scored by an experienced hepatopathologist, who was blinded to the study results. Sections were scored for macrovesicular steatosis grade, inflammation, fibrosis, and ballooning according to the NASH Clinical Research Network scoring system defined by Kleiner et al. 2005 (20).

Percentage of steatosis was graded as follows: none (0–5%), mild (5–33%), moderate (33–66%), and severe (> 66%). To assess the severity of NAFLD/NASH, the NAFLD activity score (NAS) was calculated [Kleiner et al, 2005]. The NAFLD activity score is a histologic scoring system that represents the sum of scores for steatosis, lobular inflammation, and ballooning and ranges from 0 to 8. NAFLD activity scores of 0–2 are considered not diagnostic of NASH; 3 and 4 borderline for NASH and 5–8 diagnostic of NASH.

Calculations and statistical analyses

Data were analysed using parametric and non-parametric tests. For the statistical analyses of mRNA expression, the unpaired Kruskal Wallis was used. Correlations were done using the Spearman's Rho test. Patient characteristics are presented as mean ± SD. SPSS version 20.0 (SPSS, Chicago, IL, USA) was used for statistical analyses. Comparisons were considered statistically significant if the p value was <0.05 and $p < 0.1$ was considered a trend. Clamp data are presented as median [minimal - maximum]. Endogenous glucose production (EGP) and insulin-mediated peripheral glucose uptake (rate of disappearance [Rd]) were calculated using the modified form of the Steel equation as described previously (21, 22). EGP is expressed as μmol/kg fat-free mass (FFM)*min^{-1} and Rd as μmol/kg*min^{-1}. HOMA-IR was calculated as fasting glucose x fasting insulin divided by 22.5 and quantitative insulin sensitivity check index (QUICKI) as $1/[\log(I_0) + \log(G_0)]$.

Results

Study participants

Twenty morbidly obese women scheduled for RYGB surgery and six healthy lean normal glucose tolerant women, scheduled for elective cholecystectomy for benign gallbladder disease, were included (table 1).

Table 1. Patient characteristics

	LEAN (N=6)	OBESE (N=20)	P
AGE (YEARS)	36 ± 6.6	41 ± 8.5	0.203
WEIGHT (KG)	69.7 ± 5.0	127.5 ± 21.5	< 0.001
BMI (KG/M^2)	22.1 ± 1.4	45.3 ± 6.2	<0.001
HOMA-IR	1.0 ± 0.7	2.8 ± 1.2	0.002
QUICKI	0.6 ± 0.09	0.3 ±0.03	<0.001
INSULIN (PMOL/L)	31.1 ± 19.8	88 ± 32	<0.001
GLUCOSE (MMOL/L)	5.0 ± 0.4	5.6 ± 1.1	0.169
ASAT (U/L)	16.5 ± 2.9	22 ± 14.7	0.77
ALAT (U/L)	22.2 ± 9.1	17.5 ± 25.7	0.91
Γ-GT (U/L)	27.5 ± 14.3	24.5 ± 43.7	0.60
ALP (U/L)	67.8 ± 34.2	53 ± 18.9	0.38
TRIGLYCERIDES (MMOL/L)	1.3 ± 0.7	1.0 ± 0.7	0.77
HDL-CHOLESTEROL (MMOL/L)	1.5 ± 0.3	1.1 ± 0.2	<0.001
LDL-CHOLESTEROL (MMOL/L)	3.6 ± 0.7	2.8 ± 0.6	0.008
TOTAL CHOLESTEROL (MMOL/L)	5.8 ± 0.9	4.3 ± 0.7	<0.001

Data are presented as mean and SD. BMI=body mass index, AST=aspartate aminotransferase, ALT=alanine aminotransferase, γ-GT = γ-glutamyltranspeptidase, ALP=alkaline phosphatase.

Glucose Metabolism

HOMA-IR and QUICKI significantly differed between the lean and obese group (table 1). Basal glucose metabolism was assessed in 19 and insulin sensitivity in 17 obese women due to technical problems related to iv access. EGP was 13.7 [10.3- 18.1] µmol/kgFFM*min and Rd 24.6 [11.5 – 42.5] µmol/kg/min. Hepatic insulin sensitivity, expressed as insulin-mediated suppression of EGP, was assessed during the first step of the hyperinsulinemic clamp and was 78 [55-99]% (16).

IHTG

We analysed 18 obese subjects because ^{1}H-MRS measurements were not successful in two patients. One subject was claustrophobic and one scan failed due to a technical error. The interval between the ^{1}H-MRS assessment and surgery was two weeks. Mean IHTG was 7.7± 9.0% [range 0-28.8%] (fig. 1). There was no correlation between IHTG and BMI ($p = 0.184$, $r = -0.328$) or insulin-mediated EGP suppression (fig. 2) while basal EGP tended to be positively correlated to IHTG ($p = 0.073$, $r = 0.782$).

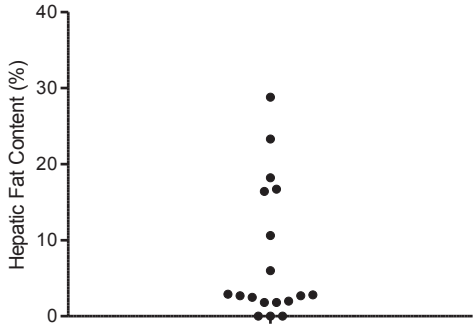

Figure 1. Scatterplot showing hepatic fat content measured with 1.0T ^{1}H-MR Spectroscopy (MRS) (n = 18).

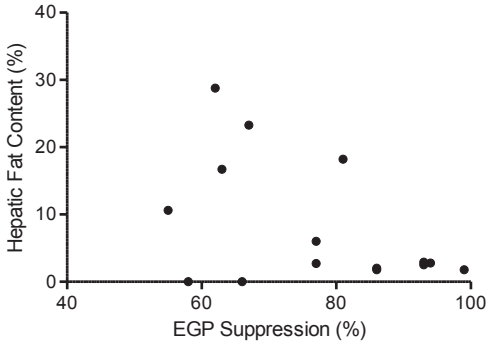

Figure 2. Correlation between hepatic fat content and insulin-mediated suppression of endogenous glucose production (r = -0.276; p = 0.290).

Liver Histopathology

Histopathology assessment of liver specimens (n = 19) showed no hepatis steatosis in 7 subjects, 9 subjects had mild macrovesicular steatosis, 1 had moderate steatosis, and 2 had severe steatosis. Hepatic steatosis assessed in the liver biopsies correlated significantly with IHTG measured with MRS (p = 0.03, r = 0.52). No lobular inflammation foci were found in 7 subjects, < 2 foci in 11 subjects and one subject showed a few ballooning cells. The NAFLD activity score was <3 in 16 subjects, 3-4 in 2 subjects and 5 in one subject.

Liver pro– and anti–inflammatory markers in lean and obese subjects

In 2 of the obese subjects the obtained frozen material was of poor quality and could not be used for further analyses. Obese subjects (n = 18) demonstrated overall increased gene expression levels of pro- and anti-inflammatory markers. Expression of the pro-inflammatory markers CD68, TNFα, CCL2 and MIP1beta and the anti-inflammatory markers IL10, MR and the scavenger receptor CD163 were significantly higher in the obese compared to the lean controls (fig. 3). In the lean group there was no correlation between QUICKI and expression of any of the inflammatory genes. In the obese subjects, the expression levels of the pro- and anti-inflammatory markers did not correlate with basal EGP or hepatic and peripheral insulin sensitivity.

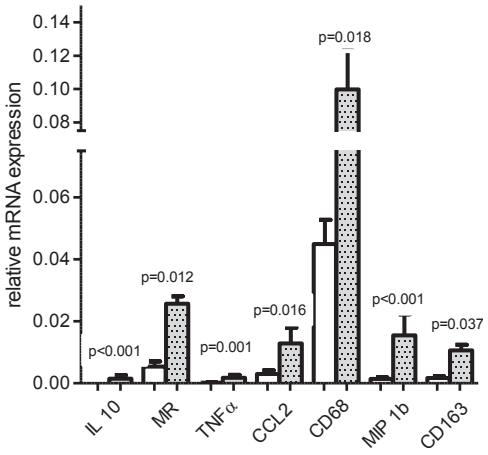

Figure 3. Inflammatory gene expression (mean ± SD) in liver tissue from obese (grey columns, n = 18) and lean (white columns, n = 6) women. Mann-Whitney test.

Inflammatory markers in subjects with and without hepatic steatosis

Hepatic fat content did not correlate with expression of liver inflammatory markers within the obese group. We next analysed the subjects with (n = 5) and without (n = 11) hepatic steatosis (cut off point 5.7% (23) separately. Interestingly, in the subjects with hepatic steatosis, a strong inverse correlation between the expression of IL-10 and IHTG was found (p = 0.004 ; r = 0.953; fig. 4) while MIP1beta showed a trend for an inverse correlation with IHTG (p = 0.059; r = 0.746). The other inflammatory markers did not correlate with IHTG in both groups. There was no significant difference in liver IL-10 expression between the subjects with or without hepatic steatosis.

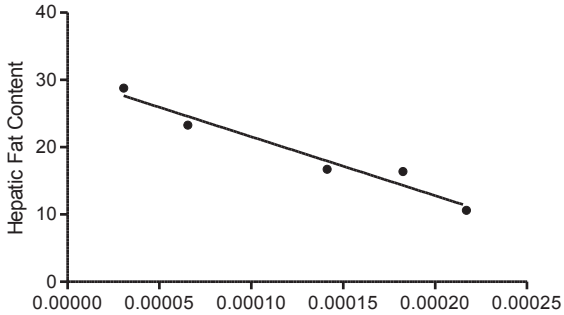

Figure 4. Correlation between relative IL10 mRNA expression and hepatic fat content (%) in liver tissue of obese subjects with hepatic steatosis (r = -1.0; p = 0.0167).

Inflammatory markers in subjects with and without hepatic insulin resistance

Within the obese group, hepatic insulin sensitivity did not correlate with gene expression levels of any of the inflammatory markers. We next studied whether the inflammatory

markers were differentially expressed when insulin-mediated suppression of EGP was below or above the median for the whole group (>79% EGP suppression). There were no significant correlations between expression of analysed inflammatory markers in liver tissue and subjects with higher or lower hepatic insulin sensitivity.

C–reactive protein

Plasma CRP was significantly higher in the obese group (obese 9489 ng/ml ± 6144 (1221-21238) vs lean 1419 ng/ml ± 521 (784-2196); $p < 0.001$). There was neither a significant correlation between IHTG and circulating CRP ($p = 0.50$; $r = 0.17$) nor between CRP and hepatic insulin sensitivity ($p = 0.11$; $r = 0.39$) in the obese group. These results did not change when analysing the hepatic insulin resistant or hepatic steatosis groups separately (data not shown).

Discussion

We studied gene expression of pro- and anti-inflammatory markers in liver tissue of morbidly obese women and matched lean controls and show that pro-inflammatory as well as anti-inflammatory markers are markedly increased in the obese group. Next we studied the association between liver fat content, hepatic and peripheral insulin sensitivity and expression of the inflammatory markers in the obese women and showed that overall, morbidly obese women are characterized by an inflamed liver independent of liver fat content or insulin sensitivity. Within the obese subgroup with hepatic steatosis, expression of the anti-inflammatory cytokine IL10 was inversely correlated with IHTG.

Obesity and high fat diets are associated with the production of cytokines in liver through an activated NFkB pathway (24). In experimental models, this inflammatory response can be triggered by excessive uptake of fatty acids leading to lipotoxicity, ER stress and reactive oxygen species (ROS) formation (25). Besides, gut-derived endotoxins, dietary derived lipids and fructose might activate Kupffer cells resulting in a pro-inflammatory phenotype. (26, 27, 28, 29)

Although it has been shown that hepatic inflammation can induce hepatic and system insulin resistance in rodents (24), no correlation was present between inflammatory markers and hepatic and peripheral insulin sensitivity in our obese subjects. In theory, this discrepancy can be explained by a species-specific phenomenon, by a difference in the magnitude of inflammatory changes or by the presence of a counterbalanced anti-inflammatory response as observed in our subjects. The origin of the increase in inflammatory proteins cannot be deducted from the current study, but in rodents it has been shown that active recruitment of monocyte-like myeloid cells expressing the CCR2 receptor occurs in response to a high fat diet resulting in obesity (15). Additionally, a high fat choline deficient diet, resulting in hepatic steatosis, increases the number of hepatic natural killer cells and activated T-cells that in turn can activate Kupffer cells and induce a proinflammatory phenotype (30). Further studies in

humans are needed to characterize the immune cells involved in obesity-associated hepatic inflammation.

Overall, our subjects did not show a correlation between gene expression of inflammatory proteins in liver and liver triglyceride content, while several earlier studies suggested that lipid accumulation in liver can trigger an inflammatory response and that liver inflammation per se can trigger hepatic steatosis through upregulation of Sterol Regulatory Element-Binding Proteins 1c (SREBP1c) and lipogenic enzymes (11, 31, 32). In line, TNFα-knock out mice on a high fat diet are protected from hepatic steatosis through reduced lipid uptake and triglyceride synthesis (33). The broad range in hepatic fat content (from none to severe steatosis) in our subjects might in part explain the lack of a significant association.

One of the included subjects had a NAS score of 5 suggesting the presence of NASH. Interestingly peripheral insulin sensitivity was lowest and basal EGP was highest in this subject. This is in line with an earlier report on the association between NASH and insulin resistance (34). Unfortunately, assessment of IHTG with 1H-MRS failed in this patient due to claustrophobia.

Studying the groups with and without hepatic steatosis separately showed a significant inverse correlation between IL-10 and IHTG. Recently it has been shown that IL-10 secreted by M2 polarized Kupffer cells in liver induces apoptosis of pro-inflammatory M1 polarized Kupffer cells (35), indicating that the M2/M1 balance in hepatic steatosis contributes to the overall inflammatory phenotype. This suggests that in patients with hepatic steatosis, IL10 serves to dampen the inflammatory response and might contribute to reducing further accumulation of liver fat since hepatic inflammation has been shown to increase de novo lipogenesis as described above.

Finally, no correlation was found between IHTG and systemic and hepatic insulin resistance. This is in line with an earlier study showing that increased hepatic triglycerides per se do not cause insulin resistance (8) and other studies showing that diacylglycerol and activated PKC are more important in the induction of hepatic insulin resistance (9, 10).

In conclusion, morbid obesity is associated with hepatic inflammation independent of liver fat content and insulin sensitivity. In hepatic steatosis, IL10 might play a pivotal role in controlling the magnitude of the pro-inflammatory phenotype and further increment of liver fat accumulation. Further studies are needed to characterize the different types of immune cells present in the liver of obese subjects.

References

1. Ferreira DM, Castro RE, Machado MV, et al. Apoptosis and insulin resistance in liver and peripheral tissues of morbidly obese patients is associated with different stages of non-alcoholic fatty liver disease. Diabetologia 2011; 54:1788–1798.

2. Anty R, Bekri S, Luciani N, et al. The inflammatory C-reactiveprotein is increased in both liver and adipose tissue in severely obese patients independently from metabolic syndrome, Type 2 diabetes, and NASH. Am J Gastroenterol 2006; 101(8):1824–33.

3. Cai D, Yuan M, Frantz DF, et al. Local and systemic insulin resistance resulting from hepatic activiation of IKK-β and NF-κB. Nature Medicine 2005; 11(2):183-190.

4. Feldstein, A. Novel insights into the pathophysiology of non-alcoholic fatty liver disease. Seminars in liver disease 2010; 30(4):391-401.

5. Cohen JC, Horton JD, Hobbs HH. Human fatty liver disease: old questions and new insights. Science 2011; 332(6037):1519-23.

6. Kabir M, Catalano KJ, Ananthnarayan S, et al. Molecular evidence supporting the portal theory: a causative link between visceral adiposity and hepatic insulin resistance. Am J Physiol Endocrinol Metab 2005; 288(2):E454-61.

7. Kotronen, A, Juurinen L, Tiikkainen M, et al. Clinical liver, pancreas and biliary tract. Gastroenterology 2008; 135:122-130.

8. Visser ME, Lammers NM, Nederveen AJ, et al. Hepatic steatosis does not cause insulin resistance in people with familial hypobetalipoproteinaemia. Diabetologia 2011; 54(8):2113-21.

9. Birkenfeld AL, Shulman GI. Nonalcoholic fatty liver disease, hepatic insulin resistance, and type 2 diabetes. Hepatology 2014; 59(2):713-23.

10. Samuel VT, Liu ZX, Wang A, et al. Inhibition of protein kinase Cepsilon prevents hepatic insulin resistance in nonalcoholic fatty liver disease. J Clin Invest 2007; 117(3):739-45.

11. Berlanga A, Guiu-Jurado E, Porras JA, et al. Molecular pathways in non-alcoholic fatty liver disease. Clin Exp Gastroenterol 2014; 7:221-39.

12. Savage DB, Semple RK. Recent insights into fatty liver, metabolic dyslipidaemia and their links to insulin resistance. Curr Opin Lipidol 2010; (4):329-36.

13. Fu S, Yang L, Li P, et al. Aberrant lipid metabolism disrupts calcium homeostasis causing liver endoplasmic reticulum stress in obesity. Nature 2011; 473(7348):528-31.

14. Jais A, Einwallner E, Sharif O, et al. Heme oxygenase-1 drives metaflammation and insulin resistance in mouse and man. Cell 2014; (158):25-40.

15. Obstfeld AE, Sugaru E, Thearle M, et al. A.W. C-C Chemokine receptor 2 (CCR2) regulates the hepatic recruitement of lyeloid cells that promote obesity-induced hepatic steatosis. Diabetes 2010; 59:916-925.

16. de Weijer BA, Aarts E, Janssen IM, et al. Hepatic and peripheral insulin sensitivity do not improve 2 weeks after bariatric surgery. Obesity 2013; 87:1143-7.

17. Ackermans MT, Pereira Arias AM, Bisschop PH, et al. The Quantification of Gluconeogenesis in Healthy Men by 2H2O and [2-13C]Glycerol Yields Different Results: Rates of Gluconeogenesis in Healthy Men Measured with 2H2O Are Higher Than Those Measured with [2-13C]Glycerol. J Clin Endocrinol Metab 2001; 86:2220-6.

18. Naressi A, Couturier C, Devos JM, et al. Javabased graphical user interface for the MRUI quantitation package. MAGMA 2001; 12:141–152.

19. Szczepaniak LS, Nurenberg P, Leonard D, et al. Magnetic resonance spectroscopy to measure hepatic triglyceride content: prevalence of hepatic steatosis in the general population. Am J Physiol Endocrinol Metab 2005; 288:E462–E468.

20. Kleiner DE, Brunt EM, Van Natta M, et al. Nonalcoholic Steatohepatitis Clinical Research Network. Design and validation of a histological scoring system for nonalcoholic fatty liver disease. Hepatology 2005; 41(6):1313-21.

21. Matthews DR, Hosker JP, Rudenski AS, et al. Homeostasis model assessment: insulin resistance and beta-cell function from fasting plasma glucose and insulin concentrations in man. Diabetologia 1985; 28:412–419.

22. Steele R. Influences on glucose loading and of injected insulin on hepatic glucose output. Ann N Y Acad Sci 1959; 82:420-30:420-430.

23. van Werven JR, Schreuder TC, Aarts EO, et al. Hepatic steatosis in morbidly obese patients undergoing gastric bypass surgery: assessment with open-system 1H-MR spectroscopy. AJR Am J Roentgenol 2011; 196(6).

24. Cai D, Yuan M, Frantz DF,et al. Local and systemic insulin resistance resulting from hepatic activation of IKK-beta and NF-kappaB. Nat Med 2005; 11:183–190.

25. Hotamisligil G.S. Inflammation and metabolic disorders. Nature 2006; 444: 860-867.

26. Basaranoglu M, Basaranoglu G, Sabuncu T, et al. Fructose as a key player in the development of fatty liver disease. World J Gastroenterol 2013; 19(8):1166-72.

27. Nagy LE. Recent insights into the role of the innate immune system in the development of alcoholic liver disease. Exp Biol Med2003; 228;882-890.

28. Dandona P, Aljada A, Bandyopadhyay A. Inflammation: the link between insulin resistance, obesity and diabetes. Trends Immunol 2004;25(1):4–7.

29. Ley RE, Turnbaugh PJ, Klein S, et al. Microbial ecology: human gut microbes associated with obesity. Nature 2006; 444(7122):1022-3.

30. Wolf MJ, Adili A, Piotrowitz K, et al. Metabolic activation of intrahepatic CD8+ T cells and NKT cells causes nonalcoholic steatohepatitis and liver cancer via cross-talk with hepatocytes. Cancer Cell 2014; 26(4):549-64.

31. Mei M, Zhao L, Li Q, et al. Inflammatory stress exacerbates ectopic lipid deposition in C57BL/6J mice. Lipids Health Dis 2011; 10:110.

32. Liu L, Mei M, Yang S, et al. Roles of chronic low-grade inflammation in the development of ectopic fat deposition. Mediators Inflamm 2014; 2014:418185.

33. Salles J, Tardif N, Landrier JF, et al. TNFα gene knockout differentially affects lipid deposition in liver and skeletal muscle of high-fat-diet mice. J Nutr Biochem 2012; 23(12):1685-93.

34. Armstrong MJ, Hazlehurst JM, Hull D, et al. Abdominal subcutaneous adipose tissue insulin resistance and lipolysis in patients with non-alcoholic steatohepatitis. Diabetes Obes Metab 2014; 16(7):651-60.

35. Wan J, Benkdane M, Teixeira-Clerc F, et al. M2 Kupffer cells promote M1 Kupffer cell apoptosis: a protective mechanism against alcoholic and nonalcoholic fatty liver disease. Hepatology 2014; 59(1):130-42.

Supplemental table

Primers used:
CD68 forward primer 5'-GCTGGCTGTGCTTTTCTCG-3', reverse primer 5'-GTCACCGTGAAGGATGGCA-3' (NM_001251; 197–307); TNFα forward primer 5'-GGCGTGGAGCTGAGAGATA-3', reverse primer 5'-CAGCCTTGGCCCTTGAAGA-3' (NM_000594; 515–603); IL10 forward primer 5'-TGCCTTCAGCAGAGTGAAGACTT-3', reverse primer 5'-TCCTCCAGCAAGGACTCCTTTA-3' (NM_000572; 197–277). MCP-1/CCL2 forward primer 5'-CCTAGCTTTCCCCAGACACC-3', reverse primer 5'-CCCAGGGGTAGAACTGTGG-3'; MR forward primer 5'-TGCAGAAGCAAACCAAACCT-3', reverse primer 5'-CAGGCCTTAAGCCAACGAAACT-3'; MIP-1β/CCL4 forward primer 5'-GCGTGACTG-TCCTGTCTCTCC-3', reverse primer 5'-ACCACAAAGTTGCGAGGAAGC-3'; CD163 forward primer 5'-ACATAGATCATGCATCTGTCATTTG-3', reverse primer 5'-ATTCTCCTTGGAATCTCACTTCTA-3'